LEARNING TO EXPLORE AND EXPLOIT WITH GNNS FOR UNSUPERVISED COMBINATORIAL OPTIMIZATION

Anonymous authors
Paper under double-blind review

ABSTRACT

Combinatorial optimization (CO) problems are pervasive across various domains, but their NP-hard nature often necessitates problem-specific heuristic algorithms. Recent advancements in deep learning have led to the development of learning-based heuristics, yet these approaches often struggle with limited search capabilities. We introduce Explore-and-Exploit GNN (X^2GNN, pronounced x-squared GNN), a novel unsupervised neural framework that combines exploration and exploitation for combinatorial search optimization: i) Exploration - X^2GNN generates multiple solutions simultaneously, promoting diversity in the search space; (ii) Exploitation - X^2GNN employs neural stochastic iterative refinement, where sampled partial solutions guide the search toward promising regions and help escape local optima. X^2GNN employs neural stochastic iterative refinement to exploit partial existing solutions, guiding the search toward promising regions and helping escape local optima. By balancing exploration and exploitation X^2GNN achieves superior performance and generalization on several graph CO problems including Max Cut, Max Independent Set, and Max Clique. Notably, for large Max Clique problems, X^2GNN consistently generates solutions within 1.2% of optimality, while other state-of-the-art learning-based approaches struggle to reach within 22% of optimal. Moreover, X^2GNN consistently generates better solutions than Gurobi on large graphs for all three problems under reasonable time budgets. Furthermore, X^2GNN exhibits exceptional generalization capabilities. For the Maximum Independent Set problem, X^2GNN outperforms state-of-the-art methods even when trained on smaller or out-of-distribution graphs compared to the test set. Our framework offers a more effective and flexible approach to neural combinatorial optimization, addressing a key challenge in the field and providing a promising direction for future research in learning-based heuristics for combinatorial optimization.

1 INTRODUCTION

Combinatorial optimization (CO) problems aim to find a discrete solution that optimizes an objective function from a discrete set of feasible solutions constrained by specific problem parameters. These optimization problems frequently emerge in commercial, governmental, and scientific contexts, prompting extensive study in fields such as mathematics, computer science, and operations research. Many combinatorial optimization problems are NP-hard, indicating no polynomial-time exact algorithm exists unless P = NP.

Exact algorithms, which achieve optimality by implicitly or explicitly considering all possible solutions, are typically only tractable for small instances due to their exponential worst-case time complexity. Consequently, another body of work focuses on heuristic algorithms that quickly attain high-quality solutions without optimality guarantees. Work here seeks to balance computational time and solution quality, often exploring the search space through multiple different solutions, and exploiting promising ones (Eiben and Schippers, 1998).

Heuristics are often hand-crafted for a specific problem, exploring problem intricacies to achieve peak performance for a given problem distribution, requiring time and domain expertise. The rise of deep learning has enabled new learning-based heuristics that can be automatically tuned for performance using data. However, current approaches are often limited in their search capabilities, often only

iteratively improving a single solution, or naively restarting and forgetting previously generated solutions.

In this paper, we introduce **Explore-and-Exploit GNN** (**X^2GNN**, pronounced X-squared GNN), a novel unsupervised neural combinatorial optimization framework. X^2GNN combines effective exploration of the solution space with intelligent exploitation of partial solutions.

Our Main Contributions are:

1. We propose **X^2GNN**, which combines exploration and exploitation for combinatorial search optimization: (i) Exploration - X^2GNN simultaneously generates multiple coupled solutions, promoting diversity in the search space; (ii) Exploitation - X^2GNN employs neural stochastic iterative refinement to exploit partial existing solutions, guiding the search toward promising regions and helping escape local optima.
2. State-of-the-art performance: X^2GNN outperforms existing learning-based approaches on benchmark datasets for the maximum cut, maximum independent set, and maximum clique problems. Additionally, X^2GNN is competitive with general OR approaches like Gurobi, and problem specific heuristics like KaMIS, offering improved or comparable solution quality at similar time cutoffs.
3. Strong generalization capabilities: X^2GNN generalizes graphs that are out-of-distribution or up to 4 times larger than those seen during training, while still significantly outperforming other learning-based methods trained on the same distribution as the test set.
4. Rigorous Evaluation: We enhance existing benchmark datasets commonly used in the ML for combinatorial optimization community by including strong traditional baselines and evaluating solvers at comparable runtimes. We additionally allow solvers a 30-minute timelimit, which is at least 24 times longer than our longest-running model.

2 Related Work

The broad intersection between machine learning (ML) and combinatorial optimization (CO) has seen much work with different facets explored in various surveys (Bengio et al., 2021; Kotary et al., 2021; Cappart et al., 2023). State-of-the-art learning-based primal heuristics specifically can be broadly categorized by their training supervision and solution construction methods. Supervised learning approaches use training data composed of problem instances and corresponding solutions derived from existing solvers (Khalil et al., 2016; Selsam et al., 2019; Nair et al., 2020; Sun and Yang, 2023). However, these may face challenges such as the unavailability of high-quality solvers for all problems and poor generalization capabilities across different problem instances (Yehuda et al., 2020). Despite these challenges, recent studies have shown that diffusion-based training can enhance generalization in supervised learning (Sun and Yang (2023)).

Unsupervised learning approaches have also been explored, differing primarily in whether solutions are constructed autoregressively or not. Earlier non-autoregressive models generate a 'soft' solution in a single step, which is then decoded into a final solution using methods ranging from simple greedy (Karalias and Loukas, 2020) decoding to more sophisticated techniques (Min et al., 2022). As Sanokowski et al. (2024) noted, these approaches can be classified as single-step diffusion methods. These models are notably faster and more scalable than their autoregressive counterparts. Sanokowski et al. (2023) suggest that non-autoregressive solution construction may fail to capture essential dependencies among problem variables and they refer to these types of methods as mean-field approximations.

The earlier single-step non-autoregressive methods are outperformed by autoregressive construction governed by MDPs (Sanokowski et al., 2023; Zhang et al., 2023). However, these models are trained using reinforcement learning (RL) and face high computational needs and poor generalization (Sun and Yang, 2023). Additionally, autoregressive construction does not allow modification of fixed decisions, unlike diffusion-based construction where all variables can be altered at each step.

The success of generative diffusion models (Sohl-Dickstein et al., 2015) made it appealing for CO. For diffusion-based CO approaches, noise is sequentially added to the optimal solution obtained from other solvers in the forward process, and the model learns to iteratively remove this noise in the reverse process. Sun and Yang (2023) models the CO problems as a discrete diffusion problem

using Bernouilli and Categorical noise. For MIS, they outperform non-autoregressive models but have similar performance to autoregressive models, suffering from long diffusion schedules. Li et al. (2023) follow the same training procedure as Sun and Yang (2023) but employ gradient-guided noising-denosing rounds during inference. This improves upon Sun and Yang (2023); however, long diffusion schedules and reliance on the gradients hinder effectiveness. Sanokowski et al. (2024) trains a diffusion model to sample from the Boltzmann distribution with the probability of sampling a solution being positively correlated to its objective value. They derive an unsupervised loss function using a continuous Lagrangian relaxation, showing that longer generation schedules increase quality.

3 PRELIMINARIES

We consider the broad class of combinatorial optimization problems on graphs and instantiate X^2GNN for three NP-hard problems on undirected unweighted graphs $G = (V, E)$. As in many real-world scenarios, we consider distributional versions of these problems, where we are asked to train an algorithm on a dataset of instances and then deploy the algorithm on unseen instances.

Maximum Clique (MC): A clique in a graph G is a subset of vertices where every two vertices are adjacent. The Maximum Clique problem involves finding the largest clique in G.

Maximum Independent Set (MIS): An independent set in a graph G is a subset of vertices, none of which are adjacent. The Maximum Independent Set problem aims to find the largest independent set.

Maximum Cut (MCut): For a graph $G = (V, E)$, the Maximum Cut problem seeks to partition the set of nodes V into two subsets S and $V \setminus S$, maximizing the number of edges between S and $V \setminus S$.

Solutions for these problems can be represented by a binary decision for each node, $Y \in \{0, 1\}^{|V|}$, indicating solution inclusion, $Y_i = 1$ if $v_i \in S$ otherwise 0. Additionally, the maximum clique and maximum independent set problems are closely related; a clique S in graph corresponds to an independent set S in its complementary graph (Cormen et al. (2001)). We use this relationship for all approaches and solve MC problems by solving MIS on the corresponding complementary graph.

4 X^2GNN FRAMEWORK

X^2GNN, illustrated in Figure 1, is an iterative framework that explores the search space by simultaneously generating a pool of K-Coupled solutions and exploiting promising ones via stochastic refinement. K-Coupled solutions is a group of K solutions that are built collectively, we refer to each group as a K-Couple. We model the K-Couple using a multilayer graph, copying the original graph K times to represent the K solutions, and adding auxiliary edges between corresponding nodes in different layers. We model the solution values themselves as node features. We then iteratively feed the K-Couple into a graph neural network (GNN) which makes a prediction on each node corresponding to a new K-Couple. We train the GNN's outputs at each iteration using a combination of an unsupervised optimization loss, a constraint satisfaction loss, and a diversity loss on the K-Couple. Importantly, before feeding a K-Couple as input to the GNN, we randomly perturb the solution to help escape local equilibria. Furthermore, we randomly initialize the K-Couple.

Formally, given a problem represented by graph $G = (V, E)$, we represent the GNN input of K solutions at iteration t using ${}^tX \in [0, 1]^{K \times |V|}$, with ${}^tX_u^k$ denoting the feature of node $u \in V$ for solution $k \in 1, \ldots, K$ in iteration t. We use ${}^t\hat{Y}$ to denote the K-Coupled solution generated at iteration t. That is, ${}^t\hat{Y} = g_\theta(G, {}^tX)$. Similarly, we use the notation ${}^t\hat{Y}_u^k$ to denote the probability of node $u \in V$ being in solution $k \in 1, \ldots, K$ generated at iteration t.

Solution Generation and Stochastic Iterative Refinement: We refer to the first iteration ($t = 1$) of X^2GNN as construction and the subsequent iterations ($t \geq 2$) as refinement. During construction, we randomly initialize node features ${}^1X_u^k$ to 0.5 with probability p and 0 with probability $1 - p$, with p being 0.95 in practice. Essentially, we initialize the K-Couple with unbiased solutions while introducing diversity to break symmetries for nodes with identical degrees.

During refinement, we randomly set the previous iteration's output ${}^{t-1}\hat{Y}$ to 0 with probability ϕ to generate new node features ${}^tX$. The parameter ϕ offers a natural way to control exploration and exploitation. If $\phi = 1$, no information from the previous iteration is used, maximizing exploration.

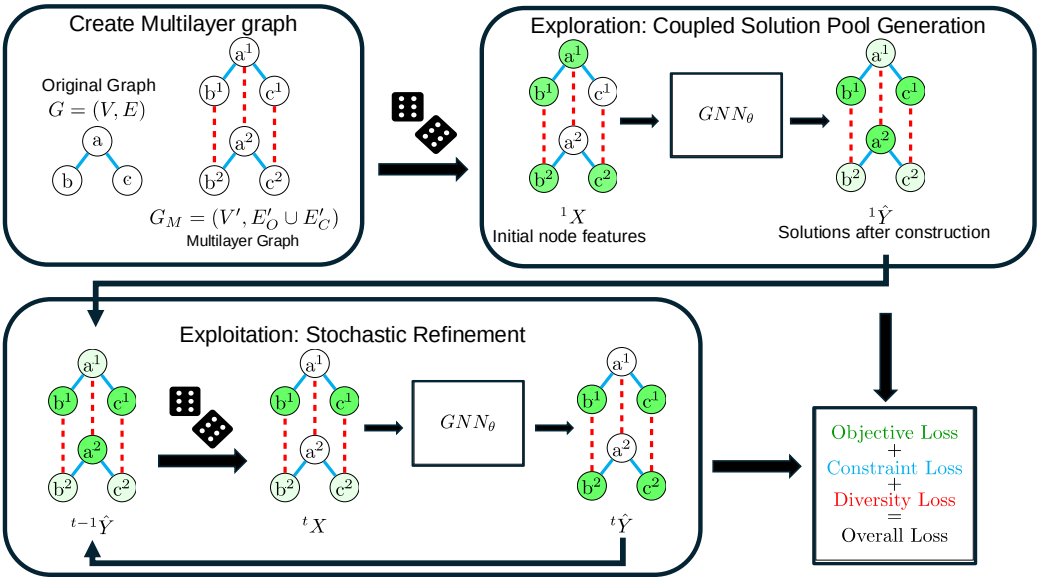

Figure 1: Illustration of X^2GNN for a Minimum Independent Set instance. First, a multilayer graph is created from $K = 2$ copies of the original graph, with cross edges to couple solutions. Copies of the original edges (E'_O) are drawn in blue, and cross edges (E'_C) are drawn in red. Node features correspond to the probability of being in the solution, representing soft solutions. Initially, when generating the coupled solutions, the features are random. These features are fed into a GNN to obtain K soft solutions. During stochastic refinement, the GNN iteratively takes solutions from the previous time step, randomly perturbs them, and generates new solutions. Stochastic refinement can be repeatedly applied at inference and is done once during training. Finally, the training loss is calculated for all generated solutions using the objective value, lagrangian term, and diversity.

If $\phi = 0$, the previously generated solutions are maintained, and the method will deterministically refine the K-Couple, maximizing exploitation. Thus, high values of ϕ lead to exploration whereas low values lead to exploitation. We refer to one step of this approach as Stochastic Refinement and the general application of multiple iterations as Stochastic Iterative Refinement.

Aligning the model's input and output enables repeated use of the recurrent model. Recurrent models trained on short iterations can be deployed for longer iterations to solve more complex problems (Schwarzschild et al., 2021); however, overuse can result in 'overthinking' (Bansal et al., 2022). X^2GNN mitigates this by not iterating over the hidden representations, but rather iterating stochastically over the output space. The stochastic sampling process significantly impacts performance by facilitating exploration around the current solution, allowing exploitation, and escaping local optima. Moreover, it helps generalization to bigger and out-of-distribution datasets.

Converting Soft Solutions to Hard Solutions: Since the GNN outputs soft solutions $\hat{Y}^k$, we convert them to discrete feasible solutions S depending on the problem. For MCut, we select a node u into S iff $\hat{Y}^k \geq 0.5$, yielding a feasible solution due to the absence of constraints. For MIS and MC, we add node u into S in order of decreasing probability $\hat{Y}^k_u$ as long as $S \cup \{u\}$ satisfies problem constraints.

***K*-Coupled Solutions:** To couple solutions, we construct a multilayer graph $G_M = (V', E')$ from the original graph $G = (V, E)$. G_M contains K "layers" each containing a copy of the original graph. Additional edges (cross edges) connect nodes in different layers corresponding to the same node in G. We denote E'_O as the edges corresponding to original edges E, and E'_C as the cross edges, such that $E' = E'_O \cup E'_C$. We construct G_M as follows: For each node $v_i \in V$, we create node v_i^k for all layers $k = 1, \ldots, K$. For each edge $(v_i, v_j) \in E$, we create an original edge between v_i^k and v_j^k for all $k = 1, \ldots, K$, forming E'_O. We then add cross edges E'_C, such that for each node $i \in V$ all copies of i have a pairwise edge between them in G_M In practice, we select $K = 2$.

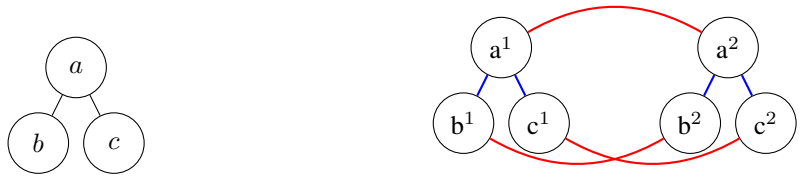

(a) Original Graph (b) Multilayer Graph with blue original edges E'_O, and red cross edges E'_C.

Figure 2: Figure shows an example of a graph and its corresponding multilayer graph for $K = 2$.

X^2GNN Neural Network Architecture: The GNN used by X^2GNN to construct and refine solutions consists of $2L$ layers combining Graph Isomorphism Networks (GIN) (Xu et al., 2019) and Graph Attention Networks (GAT) (Velickovic et al., 2018; Brody et al., 2022). The layers alternate between GIN layers operating on (V', E'_O) to work on individual solutions and GAT layers operating on (V', E'_C) to enable information sharing between solutions. This alternating design enables the simultaneous generation of K-coupled solutions. Note that the same model parameters are used for both construction and refinement.

Training and Loss Functions: We train X^2GNN using unsupervised combinatorial optimization losses which take the form of Lagrangian relaxations of the original problem. We adopt nonlinear programming formulations for MCut, MIS, and MC problems from Sanokowski et al. (2024). For MIS and MC, the objective is to include as many nodes in S as possible, penalizing constraint violation, whereas in MCut the objective is to include as many edges in the cut as possible. We additionally propose adding a loss function to promote diversity among the K-coupled solutions. In the MIS and MC settings, we want solutions to contain different nodes, whereas we are interested in having different cut edges for MCut. We write the optimization problems, continuous relaxations, and lagrangian terms for the constraints in Table 1.

Overall, X^2GNN trains the GNN parameters θ to jointly optimize objective quality ($\mathcal{L}_o$), constraint satisfaction ($\mathcal{L}_c$), and solution diversity ($\mathcal{L}_d$) over the training set $\mathcal{G}$:

$$\min_\theta \mathbb{E}_{G\in\mathcal{G}}\left[\sum_t\left[\sum_k \mathcal{L}_o(G, {}^t\hat{Y}^k) + \lambda_1\mathcal{L}_c(G, {}^t\hat{Y}^k)\right] + \lambda_2\mathcal{L}_d(G, {}^t\hat{Y})\right]$$

For MC and MIS, we impose node diversity:

$$\mathcal{L}_d(G, \hat{Y}) = \frac{1}{K(K-1)} \sum_{\substack{1\le k_1,k_2\le K\\ k_1\neq k_2}} \sum_{u\in V} \hat{Y}_u^{k_1}\hat{Y}_u^{k_2}$$

For MCut, we impose cut edge diversity:

$$\mathcal{L}_d(G, \mathcal{Y}) = \frac{1}{K(K-1)} \sum_{\substack{1\le k_1,k_2\le K\\ k_1\neq k_2}} \sum_{(u,v)\in E} \frac{1-(2\hat{Y}_u^{k_1}-1)(2\hat{Y}_v^{k_1}-1)}{2}\,\frac{1-(2\hat{Y}_u^{k_2}-1)(2\hat{Y}_v^{k_2}-1)}{2}$$

We train X^2GNN using a two-stage training procedure. In the first stage, the model learns to construct solutions, and in the second stage, the model learns to stochastically refine constructed solutions for one step. The proposed two-stage training procedure leads to better initial solutions and more stable solution refinement for X^2GNN.

Inference: Unlike during training, during inference we use the stochastic refinement step multiple times leading to stochastic iterative refinement. Training the model on a single stochastic refinement iteration is enough to teach the model to generally improve solutions. We show that using the stochastic iterative refinement longer leads to a significant increase in solution quality. Additionally, instead of generating just one K-coupled solution, we generate C K-coupled solutions to increase exploration. These K-coupled solutions are independent and effectively run X^2GNN simultaneously with different random seeds.

X^2GNN offers time-quality trade-offs by selecting C, the number of K-Coupled solutions, and T the number of iterations. By increasing C and/or T, we can consider more solutions to improve

Problem	Formulation	Objective	Constraint loss
MC	$\max_{Y \in \{0,1\}^{\lvert V \rvert}} \sum_{u \in V} Y_u$ s.t. $Y_u Y_v = 0,\ \forall (u,v) \notin E$	$\sum_{u \in V} \hat{Y}_u$	$\sum_{(u,v) \notin E} \hat{Y}_u^k \hat{Y}_v^k$
MIS	$\max_{Y \in \{0,1\}^{\lvert V \rvert}} \sum_{u \in V} Y_u$ s.t. $Y_u Y_v = 0,\ \forall (u,v) \in E$	$\sum_{u \in V} \hat{Y}_u$	$\sum_{(u,v) \in E} \hat{Y}_u^k \hat{Y}_v^k$
MCut	$\max_{Y \in \{0,1\}^{\lvert V \rvert}} \sum_{(u,v) \in E} \frac{1-(2Y_u-1)(2Y_v-1)}{2}$	$\sum_{(u,v) \in E} \frac{1-(2\hat{Y}_u-1)(2\hat{Y}_v-1)}{2}$	–

Table 1: Mathematical formulation, objective loss $\mathcal{L}_o$, and constraint loss $\mathcal{L}_c$ for our problems.

solution quality by using more time. For each choice of C and T, X^2GNN generates $C \times K$ solutions at the first iteration that are then refined for $T-1$ iterations to generate $C \times K \times T$ solutions in total. A natural question is how to select C and T for a fixed computational budget. Under a fixed budget, increasing C promotes exploration by maintaining more solutions, whereas increasing T enhances exploitation by allowing more refinement iterations on existing solutions. This mechanism controls exploration and exploitation in our optimization framework, which is crucial for effectively navigating the search landscape of complex problems.

5 EXPERIMENTS

Datasets: Previous literature has identified that some problem instances for MIS and MC are relatively easy (Dai et al., 2020). For rigorous evaluation, we use synthetically generated hard instances for all problems, following previous work (Karalias and Loukas, 2020; Zhang et al., 2023; Sanokowski et al., 2024). Our datasets include RB graphs (Xu and Li, 2000), a revision to model B graphs (Gent et al., 2001; Smith and Dyer, 1996), which are known to generate hard instances for MC and MIS. We consider RB graphs with 200-300 nodes(RB250) and 800-1200 nodes (RB1000). For MIS, we also evaluate on Erdős-Rényi (ER) graphs (Erdös and Rényi, 1959) with 700-800 nodes and edge probability 0.15 (ER750). For MCut, we use Barabási-Albert (BA) graphs (Barabási and Albert, 1999) with 250 nodes (BA250) and 1,000 nodes (BA1000). We train on 4,000 graphs and test on 500 graphs except for ER which has 128 test graphs.

Baselines: We compare X^2GNN against both Operations Research (OR) and Machine Learning (ML) techniques. We compare against Gurobi (Gurobi Optimization, LLC, 2024) on all tasks as it is a general-purpose exact solver that is highly performant on many CO tasks due to years of development. For MIS, we compare against KAMIS (Lamm et al., 2016), a highly specialized MIS solver, as well as learning-based approaches such as PPO (Ahn et al., 2020), Gflow (Zhang et al., 2023), DIFFUSCO (Sun and Yang, 2023), T2T (Li et al., 2023), and DiffUCO (Sanokowski et al., 2024). For MC, we benchmark against KAMIS used on the complement graph, greedy algorithms, mean-field annealing (MFA), and learning-based methods including ERDOS and its annealed version ANNEAL (Karalias and Loukas, 2020; Sun et al., 2022), DiffUCO, and Gflow. MCut comparisons include semi-definite-programming (SDP) based approximation algorithm (Goemans and Williamson, 1995), Tabu Search (TS) (Nath and Kuhnle, 2024), and learning-based methods RUN-CSP (Tönshoff et al., 2020), ANYCSP (Tönshoff et al., 2023), ERDOS, ANNEAL, DiffUCO, and Gflow. When given, we use Fast, Quality, and 30min to denote that we set time limits around the twice the fastest version of X^2GNN, twice the slowest version of X^2GNN, and 30 minutes respectively.

Evaluation Metrics: We employ three metrics: the mean objective value (Size), the mean drop in quality relative to the best-known solution (Drop), and the mean runtime in seconds (Time). Overall, better methods find solutions with lower solution quality drop at smaller runtimes. Since all problems are maximization problems, larger size is better. For instance, a 10% drop means the method generates solutions with a mean objective value of 90, while the best method achieves 100. In all tables, learning-based methods are shaded. Bold entries denote the best learning-based method, and italics indicate the best method, learning or traditional. Additionally, we denote the method type categorizing methods into operations research (OR), heuristic (H), supervised learning (SL), and unsupervised learning (UL).

Table 2: Results for Max Clique on small and large RB graphs, presenting the mean clique size, drop in quality to the virtual best, and runtime in seconds. Learning-based methods are shaded and the best learning-based result is bolded. The best global result is in italics. X^2GNN generates solutions at least 14% to 23% better than all learning-based methods. X^2GNN solves RB250 optimally, with a similar run time as Gurobi and KaMIS.

Method	**Type**	**RB250**			**RB1000**		
		Size ↑	Drop ↓	Time ↓	Size ↑	Drop ↓	Time ↓
KaMIS	OR	*19.074*	*0%*	10	*40.652*	*0%*	51
Gurobi (30min)	OR	*19.074*	*0%*	0.73	*40.652*	*0%*	287
Gurobi (Quality)	OR	19.068	0.03%	0.61	36.23	10.88%	47
Gurobi (Fast)	OR	14.62	23.35%	0.17	25.36	37.62%	3
Greedy	H	13.53	29.07%	0.03	26.71	34.30%	0.04
MFA	H	14.82	22.30%	0.04	27.94	31.27%	0.21
Erdos	UL	12.02	36.98%	0.06	25.43	37.44%	0.2
Anneal	UL	14.1	26.08%	0.06	27.46	32.45%	0.2
Gflow	UL	16.24	14.86%	0.06	31.42	22.71%	0.44
DiffUCO	UL	16.3	14.54%	4.13	30.5	24.97%	7.92
X^2GNN (RB250)(2x64)	UL	19.04	0.18%	0.09	39.83	2.02%	1.5
X^2GNN (RB250)(8x64)	UL	19.072	0.01%	0.37	40.09	1.38%	5.8
X^2GNN (RB250)(32x64)	UL	***19.074***	***0%***	1.41	**40.17**	**1.19%**	23.5

For generalization, we denote the training dataset with (RB250) or (BA250) in the model name. We denote variants of X^2GNN that generate C 2-Coupled solutions and use $T - 1$ stochastic refinement steps with (2CxT) in the model name.

5.1 Results on Maximum Clique

Results for MC on small and large RB datasets are shown in Table 2. For MC, we train X^2GNN on RB250 and showcase generalization to larger instances. X^2GNN generates solutions of at least 14% and 23% higher objective value than the second best learning-based methods on RB250 and RB1000 respectively.

Compared to traditional algorithms, X^2GNN solves every instance on RB250 dataset optimally, with a similar run time as Gurobi and KaMIS. On the larger dataset, on which X^2GNN wasn't trained, X^2GNN generates solutions that are within 2% of optimality while almost being 50 and 190 times faster than KaMIS and Gurobi, respectively. Additionally, at a similar runtime, X^2GNN has substantially better solution quality than Gurobi.

5.2 Results on Max Independent Set

Table 3 presents results for Maximum Independent Set (MIS) on small RB, large RB, and ER graphs. For all datasets, the metaheuristic KaMIS achieves the best solution quality. Again, X^2GNN outperforms all learning-based methods by a large margin, especially for the largest RB1000 dataset, where X^2GNN generates solutions that are 9% better than the second best. Even the model trained on RB250 dataset is able to outperform the other learning-based methods on both RB1000 and ER750 datasets, showing that X^2GNN can successfully generalize to harder and different graph distributions.

Comparison with the traditional algorithms is more nuanced. On ER750, X^2GNN generates better solutions than both KaMIS and Gurobi when algorithms are given either 15 or 60 seconds. On RB1000, X^2GNN generates better solutions than Gurobi but slightly worse solutions than KaMIS at around 20 seconds.

5.3 Results on Maximum Cut

Results for Maximum Cut on small and large BA datasets are shown in Table 4. X^2GNN outperforms all state-of-the-art learning-based methods on both datasets. However, ANYCSP and DiffUCO notably have only slightly worse performance than X^2GNN both in terms of speed and quality. For the large dataset, X^2GNN outperforms Gurobi with a time limit of 30 minutes per instance while only using 0.2 seconds. Similarly, X^2GNN outperforms Tabu Search, finding better solutions faster.

Table 3: Results for Max Independent Set on small and large RB graphs and ER graphs, presenting the mean independent set size, drop in quality to the virtual best (KaMIS), and runtime in seconds. Learning-based methods are shaded and the best learning-based result is bolded. The best global result is in italics. X^2GNN substantially outperforms learning-based approaches on all datasets. When generalizing from small RB250 instances, X^2GNN outperforms learning-based methods trained on the larger and in-distribution problems. On ER instances, X^2GNN outperforms traditional OR approaches given similar time limits.

Method	**Type**	**RB250**			**RB1000**			**ER750**		
		Size ↑	Drop ↓	Time ↓	Size ↑	Drop ↓	Time ↓	Size ↑	Drop ↓	Time ↓
KaMIS (30min)	OR	*20.106*	*0%*	3.92	*43.218*	*0%*	381	*45.234*	*0%*	382
Gurobi (30min)	OR	*20.106*	*0%*	0.31	42.96	0.60%	550	43.62	3.57%	1800
KaMIS (Quality)	OR	*20.106*	*0%*	3.92	42.98	0.55%	18	44.84	0.87%	61
Gurobi (Quality)	OR	*20.106*	*0%*	0.42	42.25	2.24%	22.27	43.5	3.83%	120
KaMIS (Fast)	OR	20.032	0.37%	1.16	42.66	1.29%	6.5	43.46	3.92%	16
Gurobi (Fast)	OR	19.16	4.71%	0.1	38.81	10.20%	1.23	41.31	8.67%	3.62
PPO	UL	19.01	5.45%	0.15	32.32	25.22%	0.91	41.11	9.12%	2.11
GFlow	UL	19.18	4.61%	0.05	37.48	13.28%	0.4	41.14	9.05%	1.03
DIFUSCO	SL	17.68	12.07%	0.87	35.82	17.12%	41.11	40.35	10.80%	15.46
T2T	SL	18.35	8.73%	2.32	35.822	17.11%	26.55	41.37	8.54%	13.92
DiffUCO	UL	19.24	4.31%	0.42	38.87	10.06%	5	43.63	3.55%	0.71
X^2GNN(16x8)	UL	19.51	2.96%	0.034	40.53	6.22%	0.3	42.05	7.04%	0.31
X^2GNN(64x8)	UL	19.82	1.42%	0.128	41.54	3.88%	1.18	43.06	4.81%	1.07
X^2GNN(256x8)	UL	19.98	0.63%	0.5	42.19	2.38%	4.66	43.82	3.13%	3.91
X^2GNN(256x32)	UL	20.072	0.17%	1.94	42.48	1.71%	18.36	44.43	1.78%	15.26
X^2GNN(1024x32)	UL	**20.098**	**0.04%**	7.11	**42.81**	**0.94%**	74.4	**44.91**	**0.72%**	57.18
X^2GNN(RB250)(256x32)	UL	20.072	0.17%	1.94	39.28	9.1%	9.43	44.15	2.40%	7.96

Table 4: Results for Max Cut on small and large BA graphs, presenting the mean cut size, drop in quality to the virtual best, and runtime in seconds. Learning-based methods are shaded and the best learning-based result is bolded. The best global result is in italics. X^2GNN outperforms learning-based methods, but only slightly outperforms ANYCSP. Additionally, on BA1000, X^2GNN outperforms Gurobi given 30 minutes by generating better solutions in 0.2s.

Method	**Type**	**BA250**			**BA1000**		
		Size ↑	Drop ↓	Time ↓	Size ↑	Drop ↓	Time ↓
Gurobi (30min)	OR	*735.32*	*0%*	759	2966.58	0.76%	1800
Gurobi (Quality)	OR	731.99	0.45%	2.5	2931.02	1.95%	4.24
Gurobi (Fast)	OR	731.83	0.47%	0.16	2930.99	1.95%	0.66
SDP	OR	700.04	4.8%	4.2	-	-	-
Tabu Search	H	733.79	0.21%	3	2926.6	2.10%	11.5
Greedy	H	688.31	6.39%	0.02	2761.06	7.64%	0.29
MFA	H	704.03	4.26%	0.15	2833.86	5.20%	0.66
Erdos	UL	693.45	5.69%	0.07	2870.34	3.98%	0.25
Anneal	UL	696.73	5.25%	0.07	2863.23	4.22%	0.24
GFlow	UL	704.3	4.22%	0.27	2864.61	4.17%	1.95
RUN-CSP	UL	726.96	1.14%	0.78	2925.8	2.12%	10.8
ANYCSP	UL	735.12	0.03%	2.5	2988.6	0.02%	7.37
DiffUCO	UL	733.5	0.25%	2.77	2981.1	0.27%	6.6
X^2GNN(16x8)	UL	734.21	0.15%	0.08	2985.2	0.14%	0.2
X^2GNN(64x8)	UL	734.92	0.05%	0.15	2987.7	0.05%	0.48
X^2GNN(256x8)	UL	735.17	0.02%	1.2	2988.7	0.02%	1.95
X^2GNN(256x32)	UL	**735.26**	**0.01%**	4.1	***2989.3***	***0%***	7.3
X^2GNN (BA250)(256x32)	UL	**735.26**	**0.01%**	4.1	2985.5	0.13%	5.4

These results indicate that on 3 CO problems, X^2GNN outperforms neural baselines, is competitive with specialized metaheuristics like KaMIS, and improves over general solvers like Gurobi.

5.4 Ablation

In this section, we analyze the impact of K-coupled solutions for different values of K. We also measure the impact of stochastic refinement, two-stage training, and encouraging diversity.

Table 5: Effects of the parameter K on K-coupled solutions, showing $K = 2$ gives the lowest drop.

Problem	$K = 1$	$K = 2$	$K = 4$	$K = 8$
MIS	4.01%	0.43%	3.81%	9.47%
MC	0.14%	0.01%	0.21%	1.79%

Table 5 demonstrates that $K = 2$ is the optimal choice for both problems. Its impact is particularly significant for MIS, while more subtle for MC.

We evaluate the impact of ablating aspects of X^2GNN by comparing to our standard version which achieves a drop value of 0.43% on MIS. Using deterministic refinement instead of stochastic refinement significantly increases drop value to 4.97%. Training the full framework in a single stage increased drop value to 1.44%. Similarly, ignoring the diversity loss raises drop value to 1.81%. These findings highlight the cumulative benefits of our proposed techniques. The combination of $K = 2$ coupled solutions, stochastic refinement, two-stage training, and diversity loss is crucial for the superior performance of X^2GNN.

5.5 Neural Search Dynamics

For a fixed budget, X^2GNN can controllably balance exploration and exploitation by trading off the number of solution couples generated at each iteration C, with the number of iterations T taken.

Different search strategies are needed for MC and MIS due to the different feasible regions. MC requires exploration to avoid local optima, and MIS requires exploitation to improve solutions.

We showcase that different versions of X^2GNN perform as expected in these two settings, by analyzing the effects of choosing C and T for a fixed computational budget up to 1024. Figure 3 shows the drop in solution quality for various C with T being determined by the computational budget. Figure 3a shows that for MC, focusing X^2GNN on exploration (higher C) is more helpful, with $C = 64$ giving the best results. Conversely, Figure 3b shows that for MIS, focusing X^2GNN on exploitation, by taking more iterations T, is more helpful, with $C = 4$ giving the best results.

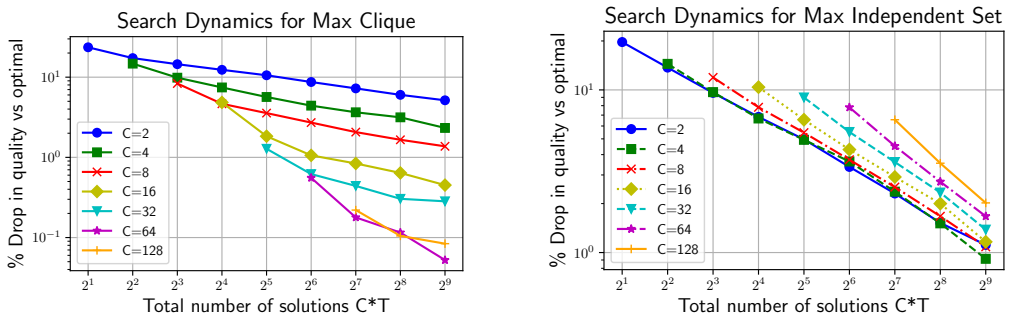

(a) (b)

Figure 3: Search dynamics on RB250: Each line corresponds to one setting of C, a parameter where higher values encourage exploration. We present the drop in solution quality (lower is better) over various computational budgets for each value of C. In MC, a problem that benefits from exploration, we see that higher values of C yield better performance. Additionally, in MIS, a problem benefiting from exploitation, we see lower values of C leading to better solutions. This indicates that C provides a meaningful lever for balancing exploration and exploitation.

6 Conclusion

In this work, we introduce Explore-and-Exploit GNN (X^2GNN), a novel unsupervised neural framework that addresses a key challenge in learning-based combinatorial optimization (CO). Unlike most existing approaches that focus on constructing a limited number of solutions, X^2GNN effectively explores the vast search space of NP-hard CO problems through two key mechanisms:

(i) Exploration: X^2GNN generates multiple solutions simultaneously, and promotes solution diversity.

(ii) Exploitation: X^2GNN employs neural stochastic iterative refinement, using sampled partial solutions to guide the search toward promising regions and escape local optima.

Our experiments on three canonical NP-Hard CO problems - Maximum Clique (MC), Maximum Independent Set (MIS), and Maximum Cut (MCut) - demonstrate that X^2GNN significantly outperforms state-of-the-art learning-based approaches. Notably, for large MC problems, X^2GNN consistently generates solutions within 1.2% of optimality, while other learning-based methods struggle to reach within 22% of optimal. Moreover, X^2GNN exhibits exceptional generalization capabilities, outperforming existing methods even when trained on smaller or out-of-distribution graphs. The iterative nature of X^2GNN allows users to trade off runtime and solution quality, as the model can be applied indefinitely to refine solutions. This feature, combined with its strong performance and generalization performance, positions X^2GNN as a competitive framework with promising directions for future research in learning-based heuristics for combinatorial optimization. By balancing exploration and exploitation, X^2GNN offers a more effective and adaptable approach to neural combinatorial optimization, addressing the limitations of existing methods and paving the way for more robust solutions to complex CO problems across various domains.

REFERENCES

Agoston E Eiben and Cornelis A Schippers. On evolutionary exploration and exploitation. *Fundamenta Informaticae*, 35(1-4):35–50, 1998.

Yoshua Bengio, Andrea Lodi, and Antoine Prouvost. Machine learning for combinatorial optimization: a methodological tour d'horizon. *European Journal of Operational Research*, 290(2):405–421, 2021.

James Kotary, Ferdinando Fioretto, Pascal Van Hentenryck, and Bryan Wilder. End-to-end constrained optimization learning: A survey. In *International Joint Conference on Artificial Intelligence*, 2021.

Quentin Cappart, Didier Chételat, Elias B Khalil, Andrea Lodi, Christopher Morris, and Petar Veličković. Combinatorial optimization and reasoning with graph neural networks. *Journal of Machine Learning Research*, 24(130):1–61, 2023.

Elias Boutros Khalil, Pierre Le Bodic, Le Song, George L. Nemhauser, and Bistra Dilkina. Learning to branch in mixed integer programming. In Dale Schuurmans and Michael P. Wellman, editors, *Proceedings of the Thirtieth AAAI Conference on Artificial Intelligence, February 12-17, 2016, Phoenix, Arizona, USA*, pages 724–731. AAAI Press, 2016. doi: 10.1609/AAAI.V30I1.10080. URL https://doi.org/10.1609/aaai.v30i1.10080.

Daniel Selsam, Matthew Lamm, Benedikt Bünz, Percy Liang, Leonardo de Moura, and David L. Dill. Learning a SAT solver from single-bit supervision. In *7th International Conference on Learning Representations, ICLR 2019, New Orleans, LA, USA, May 6-9, 2019*. OpenReview.net, 2019. URL https://openreview.net/forum?id=HJMC_iA5tm.

Vinod Nair, Sergey Bartunov, Felix Gimeno, Ingrid von Glehn, Pawel Lichocki, Ivan Lobov, Brendan O'Donoghue, Nicolas Sonnerat, Christian Tjandraatmadja, Pengming Wang, Ravichandra Addanki, Tharindi Hapuarachchi, Thomas Keck, James Keeling, Pushmeet Kohli, Ira Ktena, Yujia Li, Oriol Vinyals, and Yori Zwols. Solving mixed integer programs using neural networks. *CoRR*, abs/2012.13349, 2020. URL https://arxiv.org/abs/2012.13349.

Zhiqing Sun and Yiming Yang. Difusco: Graph-based diffusion solvers for combinatorial optimization. In A. Oh, T. Naumann, A. Globerson, K. Saenko, M. Hardt, and S. Levine, editors, *Advances in Neural Information Processing Systems*, volume 36, pages 3706–3731. Curran Associates, Inc., 2023. URL https://proceedings.neurips.cc/paper_files/paper/2023/file/0ba520d93c3df592c83a611961314c98-Paper-Conference.pdf.

Gal Yehuda, Moshe Gabel, and Assaf Schuster. It's not what machines can learn, it's what we cannot teach. In Hal Daumé III and Aarti Singh, editors, *Proceedings of the 37th International Conference on Machine Learning*, volume 119 of *Proceedings of Machine Learning Research*, pages 10831–10841. PMLR, 13–18 Jul 2020. URL https://proceedings.mlr.press/v119/yehuda20a.html.

Nikolaos Karalias and Andreas Loukas. Erdos goes neural: an unsupervised learning framework for combinatorial optimization on graphs. *Advances in Neural Information Processing Systems*, 33: 6659–6672, 2020.

Yimeng Min, Frederik Wenkel, Michael Perlmutter, and Guy Wolf. Can hybrid geometric scattering networks help solve the maximum clique problem? *Advances in Neural Information Processing Systems*, 35:22713–22724, 2022.

Sebastian Sanokowski, Sepp Hochreiter, and Sebastian Lehner. A diffusion model framework for unsupervised neural combinatorial optimization. *arXiv preprint arXiv:2406.01661*, 2024.

Sebastian Sanokowski, Wilhelm Berghammer, Sepp Hochreiter, and Sebastian Lehner. Variational annealing on graphs for combinatorial optimization. In A. Oh, T. Naumann, A. Globerson, K. Saenko, M. Hardt, and S. Levine, editors, *Advances in Neural Information Processing Systems*, volume 36, pages 63907–63930. Curran Associates, Inc., 2023. URL https://proceedings.neurips.cc/paper_files/paper/2023/file/c9c54ac0dd5e942b99b2b51c297544fd-Paper-Conference.pdf.

Dinghuai Zhang, Hanjun Dai, Nikolay Malkin, Aaron C Courville, Yoshua Bengio, and Ling Pan. Let the flows tell: Solving graph combinatorial problems with gflownets. In A. Oh, T. Naumann, A. Globerson, K. Saenko, M. Hardt, and S. Levine, editors, *Advances in Neural Information Processing Systems*, volume 36, pages 11952–11969. Curran Associates, Inc., 2023. URL https://proceedings.neurips.cc/paper_files/paper/2023/file/27571b74d6cd650b8eb6cf1837953ae8-Paper-Conference.pdf.

Jascha Sohl-Dickstein, Eric A. Weiss, Niru Maheswaranathan, and Surya Ganguli. Deep unsupervised learning using nonequilibrium thermodynamics. In Francis R. Bach and David M. Blei, editors, *Proceedings of the 32nd International Conference on Machine Learning, ICML 2015, Lille, France, 6-11 July 2015*, volume 37 of *JMLR Workshop and Conference Proceedings*, pages 2256–2265. JMLR.org, 2015. URL http://proceedings.mlr.press/v37/sohl-dickstein15.html.

Yang Li, Jinpei Guo, Runzhong Wang, and Junchi Yan. From distribution learning in training to gradient search in testing for combinatorial optimization. In Alice Oh, Tristan Naumann, Amir Globerson, Kate Saenko, Moritz Hardt, and Sergey Levine, editors, *Advances in Neural Information Processing Systems 36: Annual Conference on Neural Information Processing Systems 2023, NeurIPS 2023, New Orleans, LA, USA, December 10 - 16, 2023*, 2023.

Thomas H. Cormen, Charles E. Leiserson, Ronald L. Rivest, and Clifford Stein. *Introduction to Algorithms, Second Edition*. The MIT Press and McGraw-Hill Book Company, 2001. ISBN 0-262-03293-7.

Avi Schwarzschild, Eitan Borgnia, Arjun Gupta, Furong Huang, Uzi Vishkin, Micah Goldblum, and Tom Goldstein. Can you learn an algorithm? generalizing from easy to hard problems with recurrent networks. In Marc'Aurelio Ranzato, Alina Beygelzimer, Yann N. Dauphin, Percy Liang, and Jennifer Wortman Vaughan, editors, *Advances in Neural Information Processing Systems 34: Annual Conference on Neural Information Processing Systems 2021, NeurIPS 2021, December 6-14, 2021, virtual*, pages 6695–6706, 2021. URL https://proceedings.neurips.cc/paper/2021/hash/3501672ebc68a5524629080e3ef60aef-Abstract.html.

Arpit Bansal, Avi Schwarzschild, Eitan Borgnia, Zeyad Emam, Furong Huang, Micah Goldblum, and Tom Goldstein. End-to-end algorithm synthesis with recurrent networks: Extrapolation without overthinking. In Sanmi Koyejo, S. Mohamed, A. Agarwal, Danielle Belgrave, K. Cho, and A. Oh, editors, *Advances in Neural Information Processing Systems 35: Annual Conference on Neural Information Processing Systems 2022, NeurIPS 2022, New Orleans, LA, USA, November 28 - December 9, 2022*, 2022. URL http://papers.nips.cc/paper_files/paper/2022/hash/7f70331dbe58ad59d83941dfa7d975aa-Abstract-Conference.html.

Keyulu Xu, Weihua Hu, Jure Leskovec, and Stefanie Jegelka. How powerful are graph neural networks? In *7th International Conference on Learning Representations, ICLR 2019, New Orleans, LA, USA, May 6-9, 2019*. OpenReview.net, 2019. URL https://openreview.net/forum?id=ryGs6iA5Km.

Petar Velickovic, Guillem Cucurull, Arantxa Casanova, Adriana Romero, Pietro Liò, and Yoshua Bengio. Graph attention networks. In *6th International Conference on Learning Representations, ICLR 2018, Vancouver, BC, Canada, April 30 - May 3, 2018, Conference Track Proceedings*. OpenReview.net, 2018. URL https://openreview.net/forum?id=rJXMpikCZ.

Shaked Brody, Uri Alon, and Eran Yahav. How attentive are graph attention networks? In *The Tenth International Conference on Learning Representations, ICLR 2022, Virtual Event, April 25-29, 2022*. OpenReview.net, 2022. URL https://openreview.net/forum?id=F72ximsx7C1.

Hanjun Dai, Xinshi Chen, Yu Li, Xin Gao, and Le Song. A framework for differentiable discovery of graph algorithms. In *Learning Meets Combinatorial Algorithms at NeurIPS2020*, 2020.

Ke Xu and Wei Li. Exact phase transitions in random constraint satisfaction problems. *Journal of Artificial Intelligence Research*, 12:93–103, 2000.

Ian P Gent, Ewan MacIntyre, Patrick Prosser, Barbara M Smith, and Toby Walsh. Random constraint satisfaction: Flaws and structure. *Constraints*, 6:345–372, 2001.

Barbara M Smith and Martin E Dyer. Locating the phase transition in binary constraint satisfaction problems. *Artificial Intelligence*, 81(1-2):155–181, 1996.

P Erdös and A Rényi. On random graphs i. *Publ. math. debrecen*, 6(290-297):18, 1959.

Albert-László Barabási and Réka Albert. Emergence of scaling in random networks. *science*, 286 (5439):509–512, 1999.

Gurobi Optimization, LLC. Gurobi Optimizer Reference Manual, 2024. URL https://www.gurobi.com.

Sebastian Lamm, Peter Sanders, Christian Schulz, Darren Strash, and Renato F Werneck. Finding near-optimal independent sets at scale. In *2016 Proceedings of the eighteenth workshop on algorithm engineering and experiments (ALENEX)*, pages 138–150. SIAM, 2016.

Sungsoo Ahn, Younggyo Seo, and Jinwoo Shin. Learning what to defer for maximum independent sets. In *International conference on machine learning*, pages 134–144. PMLR, 2020.

Haoran Sun, Etash K Guha, and Hanjun Dai. Annealed training for combinatorial optimization on graphs. *arXiv preprint arXiv:2207.11542*, 2022.

Michel X Goemans and David P Williamson. Improved approximation algorithms for maximum cut and satisfiability problems using semidefinite programming. *Journal of the ACM (JACM)*, 42(6): 1115–1145, 1995.

Ankur Nath and Alan Kuhnle. A benchmark for maximum cut: Towards standardization of the evaluation of learned heuristics for combinatorial optimization. *arXiv preprint arXiv:2406.11897*, 2024.

Jan Tönshoff, Martin Ritzert, Hinrikus Wolf, and Martin Grohe. Graph neural networks for maximum constraint satisfaction. *Frontiers Artif. Intell.*, 3:580607, 2020. doi: 10.3389/FRAI.2020.580607. URL https://doi.org/10.3389/frai.2020.580607.

Jan Tönshoff, Berke Kisin, Jakob Lindner, and Martin Grohe. One model, any csp: Graph neural networks as fast global search heuristics for constraint satisfaction. In Edith Elkind, editor, *Proceedings of the Thirty-Second International Joint Conference on Artificial Intelligence, IJCAI-23*, pages 4280–4288. International Joint Conferences on Artificial Intelligence Organization, 8 2023. doi: 10.24963/ijcai.2023/476. URL https://doi.org/10.24963/ijcai.2023/476. Main Track.

DIMACS. The second dimacs implementation challenge: 1992-1993. https://iridia.ulb.ac.be/~fmascia/maximum_clique/DIMACS-benchmark. Accessed: 2024-11-20.

Martin JA Schuetz, J Kyle Brubaker, and Helmut G Katzgraber. Combinatorial optimization with physics-inspired graph neural networks. *Nature Machine Intelligence*, 4(4):367–377, 2022.

Martin JA Schuetz, J Kyle Brubaker, and Helmut G Katzgraber. Reply to: Modern graph neural networks do worse than classical greedy algorithms in solving combinatorial optimization problems like maximum independent set. *Nature Machine Intelligence*, 5(1):32–34, 2023.

William Duckworth and Michele Zito. Large independent sets in random regular graphs. *Theoretical Computer Science*, 410(50):5236–5243, 2009.

Renee Mirka and David P Williamson. An experimental evaluation of semidefinite programming and spectral algorithms for max cut. *ACM Journal of Experimental Algorithmics*, 28:1–18, 2023.

A Experimental Details

A.1 Network Architecture

We use GNN architecture where Graph Isomorphism Network (GIN) (Xu et al. (2019)) and Graph Attention Network (GAT) (Velickovic et al. (2018); Brody et al. (2022)) layers are used in an interleaved manner. We use n_L GIN and GAT layers. The initial node features (node probabilities) are transformed to a higher dimension by a linear layer before they are passed to the first GIN layer.

The GIN layers work on the original edges and GAT layers work on the crossedges. GIN layers are composed of two-layer MLPs with RELU activations after the MLP layers. We apply Batch Normalization after each MLP layer in GINs and after each GAT layer. We add skip connections to both GIN and GAT layers. Finally, the output of each GAT layer is concatenated and fed into a final two-layer MLP. This architecture is executed recurrently starting from the last hidden representation from MLP n_R times. The final output is transformed into logits and the probability that each node belongs to S is computed via Softmax. For all problems, the architecture hidden representation size is 64.

A.2 Hyperparameters

All the hyperparameters on each dataset is given in Table 6. n_L and n_R represents the number of layers and number of recurrent steps. K and C means C $K-$Coupled solutions are generated during training. On all settings, we select $K = 2$ and $C = 4$ during training. K and C values used during inference are shown right next to the model. λ_1 and λ_2 are the weights of the constraint and diversity loss, respectively.

Dataset	ep	lr	bs	n_L	n_R	h	K	C	ϕ	λ_1	λ_2
RB-250 MIS	50	0.001	64	4	2	64	2	8	0.5	1	0.75
RB-1000 MIS	50	0.001	64	4	4	64	2	8	0.5	1	0.75
ER-750 MIS	50	0.001	64	4	4	64	2	8	0.5	1	0.75
RB-250 MC	50	0.001	64	4	2	64	2	8	0.8	1	0.75
BA-250 MCut	50	0.001	64	4	2	64	2	8	0.8	-	0.75
BA-1000 MCut	50	0.001	64	4	4	64	2	8	0.8	-	0.75

Table 6: Hyperparameters used in training.

A.3 Computational Resources and Time Measurements

All experiments are conducted on a machine with 2 Intel Xeon 6348 processors with 28 cores, 1TB of memory, and 4 A100 80GB GPUs. All traditional heuristics are run using a single core and Gurobi is run with 4 cores, allowing 40GB of memory for each instance.

We only use 1 A100 during training or inference for all datasets. The training time for MIS is roughly 1 hour and 9 hours for RB250 and RB1000 datasets, respectively. The training time for MCut is roughly 1 hour and 3 hours for BA250 and BA1000 datasets, respectively. The training time for MC is roughly 2 hours for the RB250 dataset.

For baselines, we run each method in our machine and report the time we obtain on our machine to have a fair comparison. However, we use the original size when available on the same dataset split.

B ADDITIONAL EXPERIMENTS

B.1 ADDITIONAL EXPERIMENTS FOR MAXIMUM CLIQUE

For MC, we consider a challenging dataset from DIMACS implementation challenges related Maximum Clique (DIMACS). This dataset contains 37 challenging graphs. We use the X^2GNN model trained on the RB-1000 dataset as well as its fine-tuned version. We report the performance of X^2GNN 256x32 with and without fine-tuning as well as the best traditional heuristic KaMIS.

Table 7: Table shows the clique size and the running time for each instance for X^2GNN and KaMIS, considering that X^2GNN FT fine-tunes X^2GNN on these instances, and X^2GNN is trained on only RB1000 instances. The clique sizes matching the best-known solutions are shown in bold.

				Size			Runnig Time		
Instance	n	m	Best known	KaMIS	X^2GNN FT	X^2GNN	KaMIS	X^2GNN FT	X^2GNN
brock200_2	200	9,876	12	**12**	11	11	7.14	4.95	4.95
brock200_4	200	13,089	17	16	16	16	5.45	3.7	3.67
brock400_2	400	59,786	29	24	24	24	9.17	4.32	4.35
brock400_4	400	59,765	33	25	25	25	8.77	4.28	4.29
brock800_2	800	208,166	24	20	20	20	33.91	10.84	10.79
brock800_4	800	207,643	26	20	21	21	36.02	10.87	10.8
C1000.9	1,000	450,079	68	66	66	64	19.06	6.68	6.59
C125.9	125	6,963	34	**34**	**34**	**34**	5.26	3.72	3.6
C2000.5	2,000	999,836	16	15	14	0	188.80	72.63	72.4
C2000.9	2,000	1,799,532	80	75	75	73	45.28	17.67	17.59
C250.9	250	27,984	44	**44**	**44**	**44**	5.15	3.72	3.65
C4000.5	4,000	4,000,268	18	16	13	0	596.32	367.1	369.75
C500.9	500	112,332	57	56	56	55	6.88	3.8	3.74
DSJC1000_5	1,000	499,652	15	**15**	12	12	70.18	20.1	19.96
DSJC500_5	500	125,248	13	**13**	**13**	**13**	26.61	7.29	7.24
gen200_p0.9_44	200	17,910	44	**44**	**44**	**44**	5.20	3.71	3.59
gen200_p0.9_55	200	17,910	55	**55**	**55**	**55**	5.20	3.74	3.6
gen400_p0.9_55	400	71,820	55	53	**55**	**55**	5.35	3.71	3.58
gen400_p0.9_65	400	71,820	65	**65**	**65**	**65**	5.22	3.71	3.58
gen400_p0.9_75	400	71,820	75	**75**	**75**	**75**	5.65	3.75	3.58
hamming10-4	1,024	434,176	40	38	**40**	38	12.24	9.53	9.4
hamming8-4	256	20,864	16	**16**	**16**	**16**	5.76	3.66	3.55
keller4	171	9,435	11	**11**	**11**	**11**	5.40	3.71	3.58
keller5	776	225,990	27	26	23	**27**	10.97	8.32	8.26
keller6	3,361	4,619,898	59	55	39	43	61.87	75.01	75.2
MANN_a27	378	70,551	126	**126**	**126**	92	5.05	3.69	3.57
MANN_a45	1,035	533,115	345	344	343	244	5.09	3.7	3.59
MANN_a81	3,321	5,506,380	1100	**1100**	1097	664	5.06	4.25	4.14
p_hat1500-1	1,500	284,923	12	11	10	0	88.97	61.61	60.96
p_hat1500-2	1,500	568,960	65	**65**	**65**	62	85.44	39.96	40.47
p_hat1500-3	1,500	847,244	94	**94**	**94**	**94**	44.08	22.49	22.45
p_hat300-1	300	10,933	8	**8**	**8**	**8**	18.69	5.27	5.19
p_hat300-2	300	21,928	25	**25**	**25**	**25**	12.02	4.48	4.38
p_hat300-3	300	33,390	36	**36**	**36**	**36**	7.06	3.75	3.57
p_hat700-1	700	60,999	11	**11**	9	2	42.16	15.36	15.27
p_hat700-2	700	121,728	44	**44**	**44**	**44**	25.06	11.49	11.42
p_hat700-3	700	183,010	62	**62**	**62**	**62**	13.62	7.38	7.31
				3.87%	6.68%	17.41%	15.60	8.46	8.33

Table 7 shows that X^2GNN is able to generalize and generate optimal or near-optimal solutions on many instances even though it is trained on RB1000 instances, a set of much sparser instances. However, it does fail to generate good solutions on a few instances. With fine-tuning, solution quality improves quite a lot both for these failing cases and also in general, leading to an average gap of 6.68% from 17.41%. Even the most successful traditional heuristic KaMIS achieves an average gap of 3.87%. Considering this dataset is designed to be a challenging dataset, learning a general rule based on RB1000 instances that can solve many problems, and achieving a gap of 6.68% after fine-tuning is noteworthy.

B.2 ADDITIONAL EXPERIMENTS FOR MAXIMUM INDEPENDENT SET

For MIS, we evaluate X^2GNN's performance on two additional datasets. The first dataset consists of regular graphs where each node has either 3 (d=3) or 5 (d=5) neighbors. Following Schuetz et al. (2022), we generate 20 regular graphs for each degree $d \in 3, 5$ and each size n

$\in \left[10^2, 10^3, 10^4, 10^5, 10^6\right]$ for testing. For training X^2GNN, we generate 4,000 additional graphs with $n = 10^3$, enabling evaluation of both generalization and scalability.

The second dataset comprises instances from Coding Theory applications, specifically error correction codes, with graph sizes ranging from 64 to 4,096 nodes. For this dataset, we utilize the X^2GNN model trained on the RB1000 dataset. We compare against KaMIS, the state-of-the-art MIS solver, on both datasets. For the regular dataset, we additionally compare against an enhanced version of PI-GNN that uses GraphSage architecture with a penalty value of 10 (Schuetz et al., 2023).

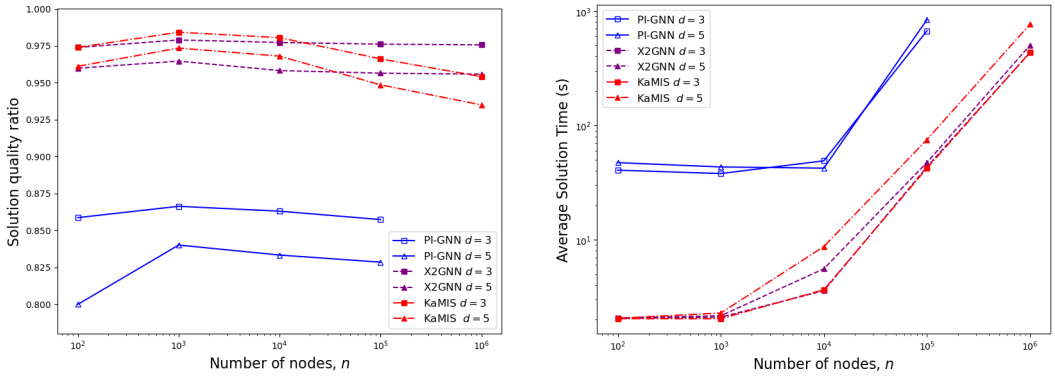

Figure 4: The plot on the left shows the relative solution quality compared to the theoretical upper bound for X^2GNN, PI-GNN and KaMIS. For this plot, higher is better. The plot on the right shows the average running time for each algorithm. For this plot lower is better. On both plots, the lines with squares and triangles show the results for regular graphs where each node has 3 and 5 neighbors, respectively. X^2GNN outperforms PI-GNN on all graph sizes and families both in terms of solution quality and runtime and outperforms KaMIS in larger graphs with a better run time.

Given the large graph sizes, obtaining optimal solutions is computationally intractable. Following Schuetz et al. (2022), we use analytical upper bounds for random d-regular graphs. The best-known bounds on the ratio α_d/n are $\alpha_3/n = 0.45537$ and $\alpha_5/n = 0.38443$ for d=3 and d=5, respectively (Duckworth and Zito, 2009). Notably, these bounds may not be tight; for n=100 and d=3 instances, both X^2GNN and KaMIS find optimal solutions (verified by Gurobi) that exhibit a 2.6% gap from the theoretical upper bound, suggesting actual performance may be better than indicated.

Figure 4 demonstrates that X^2GNN substantially outperforms PI-GNN across all problem types in both solution quality and computational efficiency. PI-GNN fails to scale to $n = 10^6$ instances due to its n^2 penalty matrix requirement, while X^2GNN handles these cases efficiently, producing high-quality solutions in approximately 500 seconds. While KaMIS slightly edges out X^2GNN on smaller instances, X^2GNN achieves superior results on larger graphs with lower computational time, demonstrating effective scaling to instances three orders of magnitude larger than those seen during training.

On the Coding Theory dataset (Table 8), X^2GNN finds the best-known solution in 20 of 32 instances, compared to KaMIS's 28 instances. X^2GNN achieves an average gap of 3.37% from best-known solutions (versus 0.34% for KaMIS). Excluding one outlier instance where X^2GNN finds a solution less than half the best-known value, X^2GNN's average gap improves to 1.74%. This performance is notable given no domain-specific tuning was performed.

To demonstrate X^2GNN's adaptability to weighted problems, we extend it to weighted maximum independent set problems with minimal modifications: adding a weight embedding layer combined with node representations via summation, and incorporating weights into the loss function calculation. Using the RB250 dataset with uniform random integer weights in between 1 and 5, we compare against optimal solutions from Gurobi. Table 9 shows X^2GNN maintains high solution quality with a 0.8% optimality gap.

In an ablation study, we replaced the GAT layer with a simple MLP for processing cross-edges. Table 10 shows this variant still outperforms other learning-based approaches but underperforms compared

Table 8: The table shows the size of the independent sets found by X^2GNN and KaMIS and the running time in seconds for each instance. The last row shows the average gap in percentages from the best-known solution. The instances where a method found the best-known solutions are shown in bold.

Graph	Best Known	X^2GNN 256x32	KaMIS	X^2GNN 256x32 Time	KaMIS Time
1dc.64	10	**10**	**10**	5.06	5.14
1dc.128	16	**16**	**16**	3.87	4.04
1dc.256	30	**30**	**30**	4.37	4.50
1dc.512	52	**52**	**52**	6.33	6.49
1dc.1024	94	**94**	93	11.29	11.40
1dc.2048	172	**172**	**172**	24.25	24.40
1et.64	18	**18**	**18**	3.81	1.31
1et.128	28	**28**	**28**	3.81	3.85
1et.256	50	**50**	**50**	3.82	3.90
1et.512	100	98	**100**	4.68	4.74
1et.1024	171	165	**171**	7.12	7.23
1et.2048	316	300	**316**	13.95	14.02
1tc.8	4	**4**	**4**	3.71	0.48
1tc.16	8	**8**	**8**	3.76	0.81
1tc.32	12	**12**	**12**	3.76	0.30
1tc.64	20	**20**	**20**	3.79	1.10
1tc.128	38	**38**	**38**	3.75	1.15
1tc.256	64	63	63	3.78	3.88
1tc.512	110	109	**110**	4.39	4.48
1tc.1024	196	189	**196**	6.64	6.73
1tc.2048	352	332	**352**	12.91	13.00
1zc.128	18	**18**	**18**	3.77	3.87
1zc.256	36	**36**	**36**	3.99	4.10
1zc.512	62	**62**	**62**	5.46	5.55
1zc.1024	112	109	**112**	9.13	9.32
1zc.2048	198	181	195	18.78	18.89
1zc.4096	379	326	353	40.19	40.41
2dc.128	5	**5**	**5**	4.52	1.46
2dc.256	7	**7**	**7**	8.22	10.06
2dc.512	11	**11**	**11**	19.07	22.31
2dc.1024	16	15	**16**	52.72	57.81
2dc.2048	24	11	**24**	152.61	162.73
Average Gap		3.37%	0.34%		

Table 9: Results for Weighted Maximum Independent Set on small RB graphs, presenting the mean independent set size, drop in quality compared to the optimal, and run time in seconds.

Method	**Type**	**RB250**		
		Size ↑	Drop ↓	Time ↓
Gurobi	OR	*82.94*	*0%*	0.21
X^2GNN(16x8)	UL	78.52	5.33%	0.03
X^2GNN(64x8)	UL	80.26	1.97%	0.09
X^2GNN(256x8)	UL	81.31	0.63%	0.35
X^2GNN(256x32)	UL	81.83	1.34%	1.25
X^2GNN(1024x32)	UL	**82.28**	**0.8%**	4.92

to the GAT version, indicating GAT's superior capability in aggregating information across different solutions.

Table 10: The results for replacing GAT layer with a MLP.

Method	**Type**	**RB250**		
		Size ↑	Drop ↓	Time ↓
KaMIS (30min)	OR	*20.106*	*0%*	3.92
Gurobi (30min)	OR	*20.106*	*0%*	0.31
KaMIS (Quality)	OR	*20.106*	*0%*	3.92
Gurobi (Quality)	OR	*20.106*	*0%*	0.42
KaMIS (Fast)	OR	20.032	0.37%	1.16
Gurobi (Fast)	OR	19.16	4.71%	0.1
PPO	UL	19.01	5.45%	0.15
GFlow	UL	19.18	4.61%	0.05
DIFUSCO	SL	17.68	12.07%	0.87
T2T	SL	18.35	8.73%	2.32
DiffUCO	UL	19.24	4.31%	0.42
X^2GNN-GAT(16x8)	UL	19.51	2.96%	0.034
X^2GNN-GAT(64x8)	UL	19.82	1.42%	0.128
X^2GNN-GAT(256x8)	UL	19.98	0.63%	0.5
X^2GNN-GAT(256x32)	UL	20.072	0.17%	1.94
X^2GNN-GAT(1024x32)	UL	**20.098**	**0.04%**	7.11
X^2GNN-MLP(16x8)	UL	18.95	5.75%	0.027
X^2GNN-MLP(64x8)	UL	19.41	3.46%	0.096
X^2GNN-MLP(256x8)	UL	19.698	2.03%	0.38
X^2GNN-MLP(256x32)	UL	19.886	1.09%	1.35

B.3 Additional Experiments for MCut

For the Maximum Cut (MCut) problem, we evaluate X^2GNN's out-of-distribution performance on two additional benchmark sets. The first dataset, introduced in Mirka and Williamson (2023), comprises diverse graphs from the SNAP Networks repository (referred to as SNAP dataset). This dataset is particularly suitable for assessing generalization capabilities due to its heterogeneous graph distributions. The second dataset, known as Gset (**?**), is a well-established benchmark collection traditionally used to evaluate MCut algorithms.

To train X^2GNN, we generate 4,000 Erdős-Rényi (ER) graphs with sizes uniformly sampled from between 200 and 500 and edge probabilities from [0.1, 0.75]. We then evaluate the trained model on both SNAP and Gset datasets.

Table 11 presents results for the SNAP dataset, comparing X^2GNN against ANYCSP (trained on the same dataset), Tabu Search (TS), Semidefinite Programming (SDP) relaxation, and BMZ heuristic from Mirka and Williamson (2023). X^2GNN discovers the best solutions among all compared methods for all but two instances, demonstrating superior performance over both ANYCSP and traditional heuristics.

For the Gset evaluation (Table 12), we use the subset specified by Schuetz et al. (2022). Comparing against results reported in their work, X^2GNN outperforms other learning-based approaches (PI-GNN and RUN-CSP) and most traditional heuristics, with only BLS achieving marginally better results when using additional stochastic refinement steps. Notably, X^2GNN 2560x36 achieves an average gap of merely 0.09% from best-known solutions, demonstrating consistent near-optimal performance across all instances.

Table 11: Table shows the cut sizes for instance and method. The cut sizes matching the best are shown in bold.

Graph	n	m	X^2GNN (256x32)	ANYCSP	TS	BMZ	SDP
ENZYMES8	88	133	**126**	**126**	**126**	**126**	**126**
johnson16-2-4	120	5460	**3036**	2941	**3036**	**3036**	**3036**
hamming6-2	64	1824	**992**	946	**992**	**992**	**992**
ia-infect-hyper	113	2196	**1279**	1208	**1279**	1278	1275
soc-dolphins	62	159	**122**	**122**	**122**	**122**	**122**
email-enron-only	143	623	**427**	**427**	**427**	426	422
dwt_209	209	976	**557**	**557**	**557**	557	551
ca-netscience	379	914	620	580	627	634	634
ia-infect-dublin	410	2765	**1771**	1709	1758	1767	1750
road-chesapeake	39	170	**126**	126	**126**	126	125
Erdos991	492	1417	**1036**	**1036**	1012	1031	1019
dwt_503	503	3265	**1938**	**1938**	1937	1931	1934
p-hat700-1	700	60999	33413	31856	33426	33440	**33450**
email-univ	1133	5451	**3775**	3764	3657	3765	3736

Table 12: Results for Max Cut on Gset dataset, presenting the cut size for each instance. The last row shows the average gap in percentages from the best solution. The best results among the learning-based methods are shown in bold.

Graph	n	m	BLS	DSDP	KHLWG	RUN-CSP	PI-GGN	X^2GNN 256x32	X^2GNN 2560x32
G14	800	4,694	*3,064*	2,922	3,061	2,943	3,026	**3,059**	**3,059**
G15	800	4661	*3,050*	2,938	*3,050*	2,928	2,990	3,043	**3,046**
G22	2,000	19,900	*13,359*	12,960	*13,359*	13,028	13,181	13,342	**13,345**
G49	3,000	6,000	*6,000*	*6,000*	*6,000*	***6,000***	5,918	***6,000***	***6,000***
G50	3,000	6,000	*5,880*	*5,880*	*5,880*	*5,880*	5,820	5,872	***5,880***
G55	5,000	*12,468*	10,294	9,960	10,236	10,116	10,138	10,249	**10,273**
G70	10,000	9,999	*9,541*	9,456	9,458	-	9,421	9,491	**9,536**
Mean Gap			0	2.21%	0.22%	-	1.39%	0.23%	0.09%